JPSE (Journal of Physical Science and Engineering), Vol. 6, No. 1, 2021, Page 10–18.
DOI: 10.17977/um024v6i12021p010

JPSE
(Journal of Physical Science and Engineering)

http://journal2.um.ac.id/index.php/jpse
EISSN: 2541-2485

# Reduced Graphene Oxide/Polyvinyl Alcohol Nanofibers Fabricated by Electrospinning Technique as An Ideal Candidate for Organic Solar Cell Devices

**Received**
18 February 2021

**Revised**
29 March 2021

**Accepted for Publication**
01 April 2021

**Published**
19 May 2021

**A Asriani[1*] and I Santoso[2]**

1. Department of Physics, Faculty of Science and Technology, UIN Alauddin Makassar, Jl. H. M. Yasin Limpo 36, Gowa, 92113, Indonesia.
2. Department of Physics, Faculty of Mathematics and Science, Universitas Gadjah Mada, Sekip Utara Bulaksumur, Yogyakarta, 55281, Indonesia.

***E-mail:** asriani.andaring@uin-alauddin.ac.id



**Abstract**
Functionalization of rGO that previously obtained by chemical reduction using hydrazine hydrate, has been done by changing its morphology into nanofiber with electrospinning technique and using PVA as a polymer matrix. The rGO nanofibers that had been formed were then characterized using Fourier Transformation-Infra Red (FTIR) spectroscopy, Scanning Electron Microscopy (SEM), and UV-Vis Spectrophotometer. FTIR spectroscopy confirmed the presence of C – C group and C = O group in nanofibers. SEM showed the change of nanofibers morphology which is marked by the increasing of fibres diameter and the hollow fibres become brighter. Furthermore, the effect of rGO concentration to nanofiber optical properties was confirmed by UV-Vis spectrophotometer. According to this characterization, the absorbance of rGO/PVA nanofiber is decreased due to increased rGO concentration. The detail of optical properties of rGO is studied through complex refractive index and dielectric constant in which Kramers-Kronig transformation is then employed to calculate complex refractive index and complex dielectric constant. From the data, the optical properties of rGO/PVA nanofibers indicating that rGO/PVA nanofibers can be applied as transparent electrode an organic solar cell devices.

**Keywords:** Reduced graphene oxide, nanofibers, electrospinning, Kramers-Kronig, organic solar cell.

## 1. Introduction

Graphene is a two-dimensional material on hexagonal honeycomb lattice consist of carbon atom with sp2 optical hybridized [1]–[3]. Graphene is known to be a very thin material with a thickness of one atom C [4]. In addition, graphene is also known to have superior properties in its electronic, thermal, and mechanical properties.

The superiority of graphene properties encourages scientists to continue to develop methods in graphene fabrication. So far, there have been many methods of producing graphene, namely exfoliation [5], [6], epitaxial growth [7], [8], chemical vapour deposition [9], [10], and chemical reduction of graphite oxide [11], [12]. Therefore, graphene in its development has had many names based on how to produce it. Reduced Graphene Oxide (rGO) is one of the derivatives of graphene obtained by reducing oxygen and hydrogen in Graphene Oxide (GO). Based on existing studies, the characteristics of rGO are almost same as the structure of graphene, generally [13]–[17].

In addition to learning how to fabricate graphene, technological advances have also encouraged researchers to explore of putative applications of graphene, such as energy storage device, sensors, organic solar cell, and many more application. In the Organic Solar Cell (OSC), graphene can be used as a transparent electrode as well as an active material layer [18]–[20]. This is because graphene is a very strong, flexible, and highly transparent material that absorbs and transmits light very well. Graphene also has an electron transport that is suitable for use in OSC. For better quality on application, graphene can be modified form into nanofibers. The form of nanofiber makes the surface area of material is increasing [21] caused by the cylinder length form with a small diameter so the amount of charge that

can be accommodated in nanofibers will increase. Therefore, it is important to know the optical properties of graphene in the nanofibers form which represented by complex refractive index and complex dielectric constant. These parameters are determined based on spectral absorbance data of UV-Vis Spectrometer test results. The absorbance data obtained is then processed by computing program using software IGOR Pro 6.36 to obtain the imaginary part of the optical constants. Since optical constants are a linear response function, they must be expressed in a complete configuration, in the form of complex composed of real and imaginary parts interconnected via Kramers-Kronig Transformation. This research aims to determine the optical properties, morphology, and functional groups of rGO/PVA nanofiber, which considered for application in organic solar cells as a transparent electrode layer.

## 2. Method

### *2.1. Sample Preparation*

Graphene in this study on rGO form. Reduced GO obtained from GO powder was subsequently chemically reduced using hydrazine hydrate [22], [23]. While, GO synthesized from graphite powder by oxidation process using Hummers method with some modification [22], [24]. The rGO powder was obtained then dispersed into 10 ml of destilled water using an ultrasonic vibrator for 3 hours with 0, 5, 10, and 15 mg of rGO. Furthermore, each solution was stirring while heated and slowly added PVA 13% wt. Once the solution is completely dissolved, the temperature was slowly lowered to room temperature with still stirring. When the temperature of the solution reaches room temperature, the stirring process was stopped. The rGO/PVA solution was then transferred to an ultrasonic vibrator and divisible for 1 hour to form a more homogeneous solution.

The last process is attaching the nanofiber rGO/PVA onto the quartz substrate using an electrospinning technique whose schematic was shown in Fig. 1. Each prepared rGO/PVA solution was inserted into a syringe with a 0.5 mm diameter needle and electrospinning at a voltage of 15 kV, the distance between the tip of the syringe and the collector as far as 15 cm for 60 seconds. The formed nanofiber was then heated using an oven at 100° C for 30 minutes to evaporate the solvent, then stored in a dry-film.

### *2.2. Characterization of rGO/PVA Nanofibers*

The optical properties of rGO/PVA nanofiber were known through absorbance data measured using Shimadzu UV1700 UV-Vis Spectrophotometer at LPPT UGM. The functional groups in nanofiber were known by characterization using the FTIR Spectrometer ABB Model MB3000 in LPPT in the range of 400–4000 $cm^{-1}$. While the morphology obtained through observation using SEM JEOL JSM 6510 in LPPT UGM.

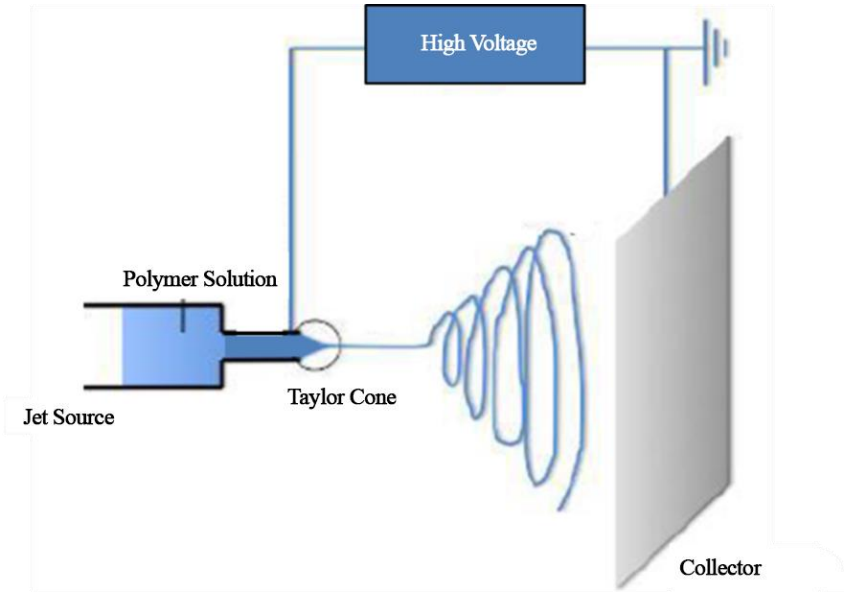


**Figure 1.** Schematic of electrospinning technique.

*2.3. Data Analyze*

The absorbance spectral data of the UV-Vis Spectrophotometer test results were then used to determine the optical quantities, including the absorption coefficient ($\alpha$), the extinction coefficient ($\kappa$), the real refractive index ($n$), and the dielectric constant ($\varepsilon$). The value of $\alpha$ can be obtained by using Equation (1).

$$\alpha = 2.303\frac{A}{d} \tag{1}$$

where $A$ is absorbance data and $d$ is nanofiber thickness data. After knowing $\alpha$, the extinction coefficient can be determined using Equation (2).

$$\kappa = \frac{\alpha\lambda}{4\pi} \tag{2}$$

with $\lambda$ representing the wavelength. The value of $\kappa$ which is the imaginary part of refractive index was used to obtain the value of the real part of refractive index $n$ by applying the Kramers-Kronig transformation relation was expressed in Equation (3) and Equation (4) [25].

$$n(\omega) = 1 + \frac{1}{\pi}P\int_{-\infty}^{\infty}\frac{\kappa(\omega')}{\omega' - \omega}d\omega' \tag{3}$$

$$\kappa(\omega) = -\frac{1}{\pi}P\int_{-\infty}^{\infty}\frac{n(\omega')}{\omega' - \omega}d\omega' \tag{4}$$

Since the Kramers-Kronig transformation requires unlimited data, whereas the measured data are only in the energy range of 1.5–6.2 eV, the first extrapolation of data at low energy to zero and at high energy (> 6.2 eV) and then interpolated to obtain the same amount of data in all samples. The extrapolated data form adjusts to two possible material properties in both extrapolation areas, minimum or maximum. Further, the extrapolated $\kappa$ data was transformed using an existing program in IGOR Pro 6.36 software to determine the value of $n$. Knowing the values of $n$ and $\kappa$, the dielectric constants $\varepsilon_1$ and $\varepsilon_2$ can be determined using Equation (5) and Equation (6).

$$\varepsilon_1 = n^2 - \kappa^2 \tag{5}$$

$$\varepsilon_2 = 2n\kappa \tag{6}$$

## 3. Result and Discussion

The success of the rGO nanofiber formed process was confirmed by the results FTIR characterization. Before being characterized, the RGO nanofiber formed into pellets. Subsequently, the sample was scanned over a wavenumber range of 600–4,000 $cm^{-1}$. This characterization provides information regarding the functional groups in the rGO / PVA nanofiber and shown in Fig. 2.

It can be seen in Fig. 2 that the nanofiber with 5 mg rGO has the same spectrum as nanofibers without rGO (0 mg). This is caused by very low rGO composition and dominated by PVA as a matrix. Differently with the higher rGO composition, which seems to have increased intensity of light that is transmitted. Thus, the existence of rGO can be ascertained in the nanofiber which causes the transparency of the nanofiber to increase. In addition, FTIR characterization displays characteristic wave peaks of a functional group that can be identified through pre-existing analysis [26]. The peaks are identified at the wavenumber around 1,041 $cm^{-1}$ which shows the presence of a C – OH alcohol group stretching vibration, peak at intermediate wavenumber around 1,616 $cm^{-1}$ and 1,720 $cm^{-1}$ respectively showed the presence of a C – C group stretching vibration and a C = O carbonyl group. From the identification results it is known that the functional groups in the nanofiber almost the same as the functional groups in rGO before being modified into nanofibers [23], except for the new peak at a wavelength of about 2,900 $cm^{-1}$. This peak indicates a C – H stretching vibration formed after morphology modification. This newly formed bond is thought to have arisen as an addition of PVA in the nanofiber. But in general, morphological changes onto nanofibers do not affect the rGO functional group.

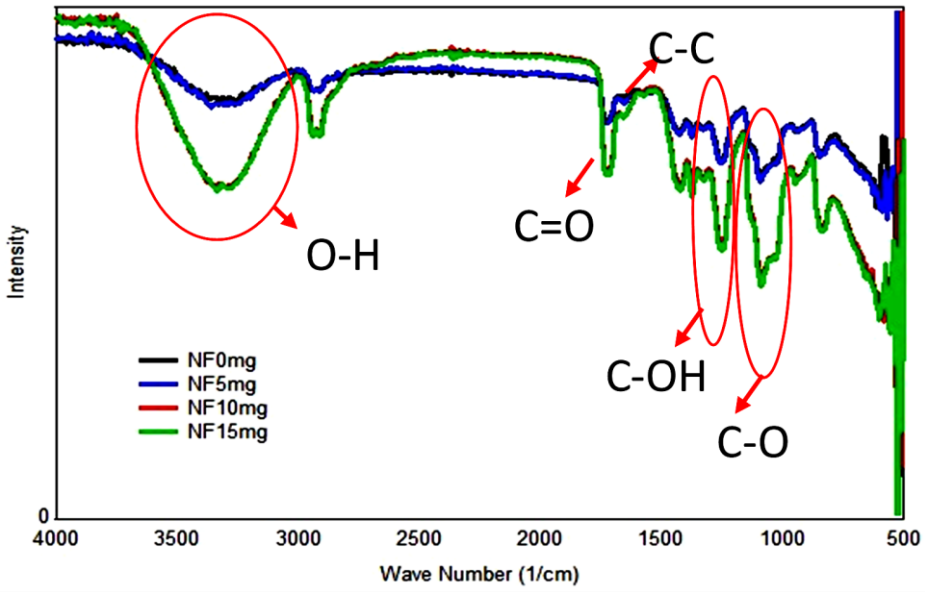


**Figure 2.** FTIR spectrum of rGO/PVA nanofibers.

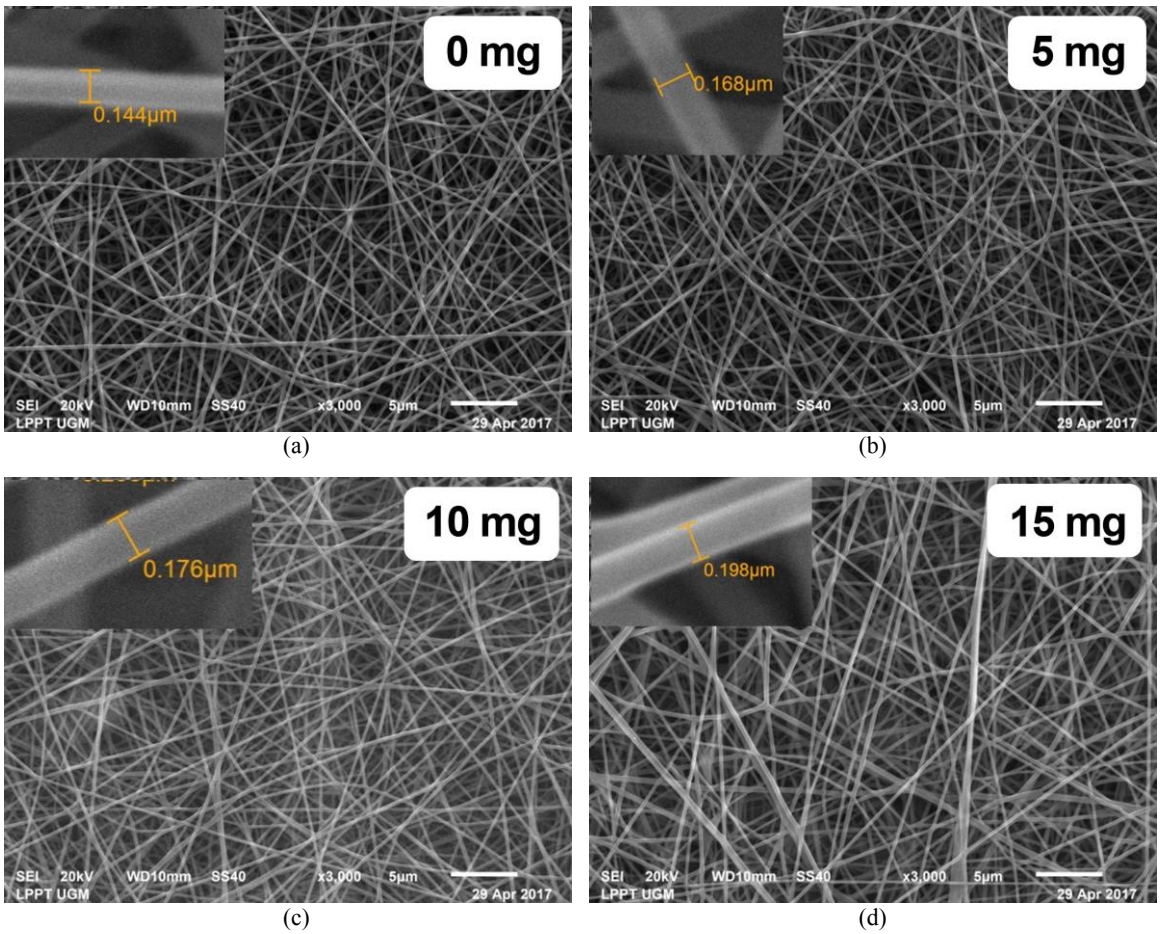


(a) (b)

(c) (d)

**Figure 3.** SEM photograph result about morphology of rGO/PVA nanofiber for (a) NF 0 mg, (b) NF 5 mg, (c) NF 10 mg, and (d) NF 15 mg.

The characteristics of the rGO/PVA nanofiber were subsequently obtained in the form of morphology characterization using SEM as shown in Fig. 3. The sample is first prepared on a metal cylinder and coated with platinum considering that the sample is an organic material with little number of free electrons. The observations obtained showed the nanofiber morphology for all samples that have been made have almost the uniform fibers. Furthermore, it is known that the addition of rGO causes the increase in fiber diameter and the hollow fiber become brighter. These results were confirmed the existence of rGO in fiber and quite similar to what has been reported by Bao *et al*. [27] and Jin *et al.* [28].

In Fig. 4, the difference in absorption curves for each nanofiber is shown significantly. The absorption spectrum of NF 0 mg is shown for comparison where the absorption only influenced by PVA. Nanofiber absorption is known at low wavelengths (< 500 nm) is inversely proportional to the increase of mass of rGO. In this case, the nanofiber becomes more transparent due to the addition of rGO mass into the nanofiber. This indicates that rGO is considered to have the same properties with graphene, which is able to transmit light up to 97.7%, contributes significantly enough in affecting the absorption of rGO nanofibers. Other than that, the addition of mass of rGO causes the absorption peak to appear wider and experience shift of the crest position to a higher wavelength, i.e. located at 275 nm wavelength. As for the shape of the peak that is getting wider due to the use of PVA as a matrix polymer thus increasing the amount of oxygen group in the rGO nanofiber.

The absorbance data obtained were then used to determine the refractive index of the imaginary part or the coefficient of extinction expressed over the energy range 1.5–6 eV, as shown in Fig. 5. Based on the curve, it is known that the value decreased significantly in the high energy range (> 2.3 eV) concomitantly with the addition of the mass of rGO. Conversely, at lower energy there are indications that the addition of more rGO mass will cause the coefficient of extinction to be higher. This is predicted that the rGO nanofiber was becoming more conductive.

In contrast to the imaginary part of refractive index profile, the real part of refractive index value obtained from numerical calculations using Kramers-Kronig transformations appears to have decreased with increasing rGO mass, as shown in Fig 6. From the calculations performed, it is known that the greater of wave energy that hits the nanofiber, the higher value of *n*. The higher *n* value indicates the bending angle of the wave electromagnetic energy which is also higher when the energy waves that pass through it greater it is.

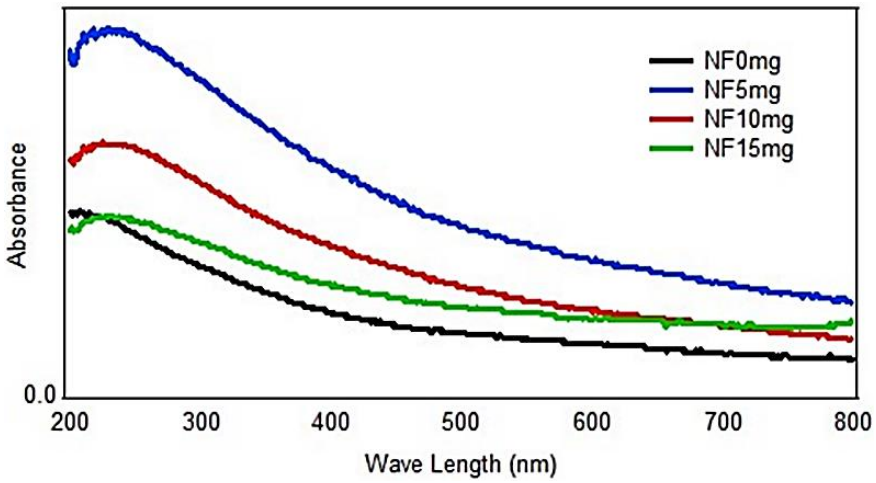


**Figure 4.** The absorbance of rGO/PVA nanofiber at various rGO mass.

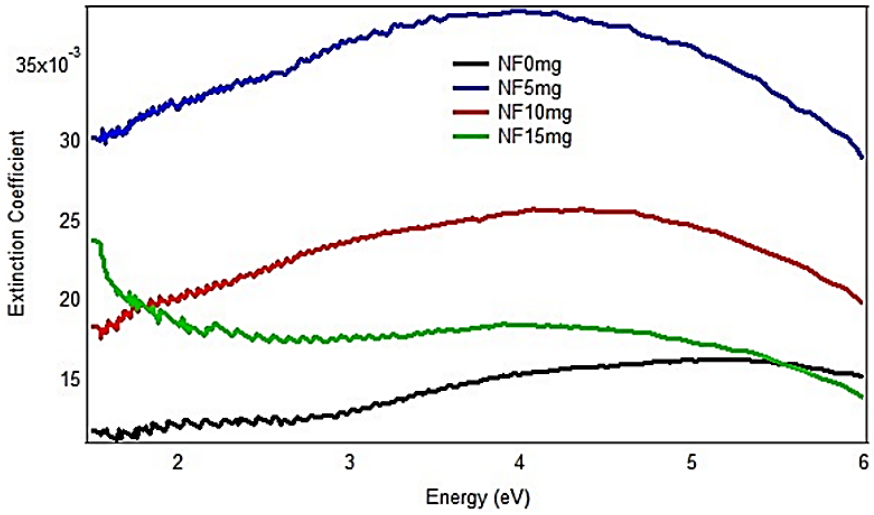


**Figure 5.** The imaginary part of the refractive index of rGO/PVA nanofiber.

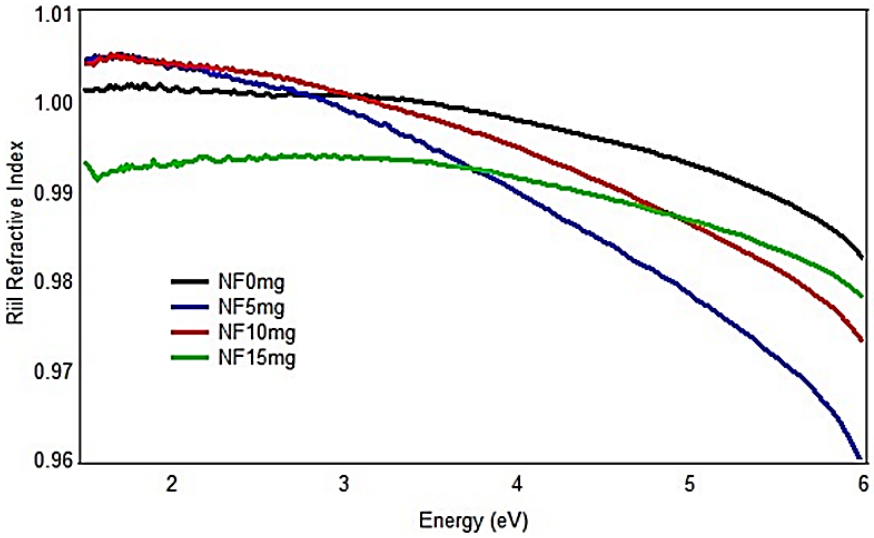


**Figure 6.** The real part of refractive index of rGO/PVA nanofiber.

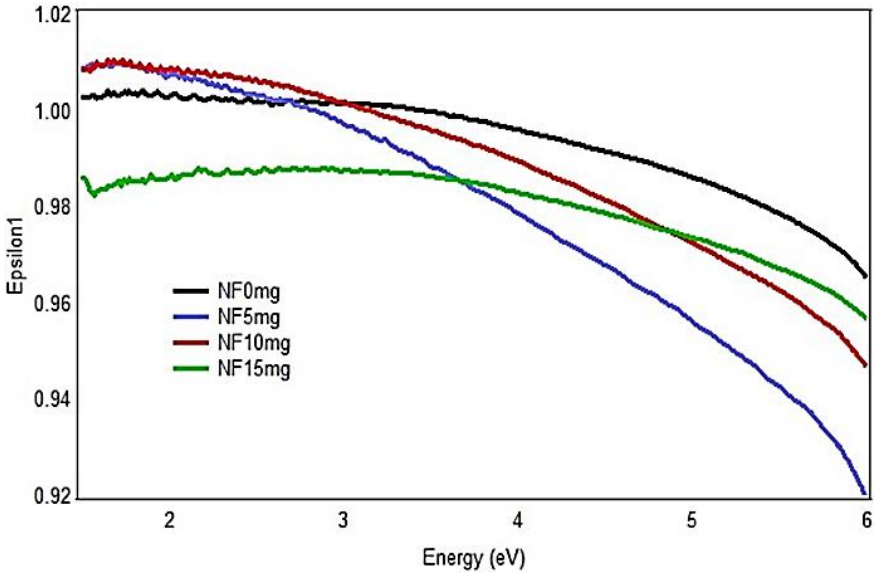


**Figure 7.** The real part of dielectric constant of rGO/PVA nanofiber.

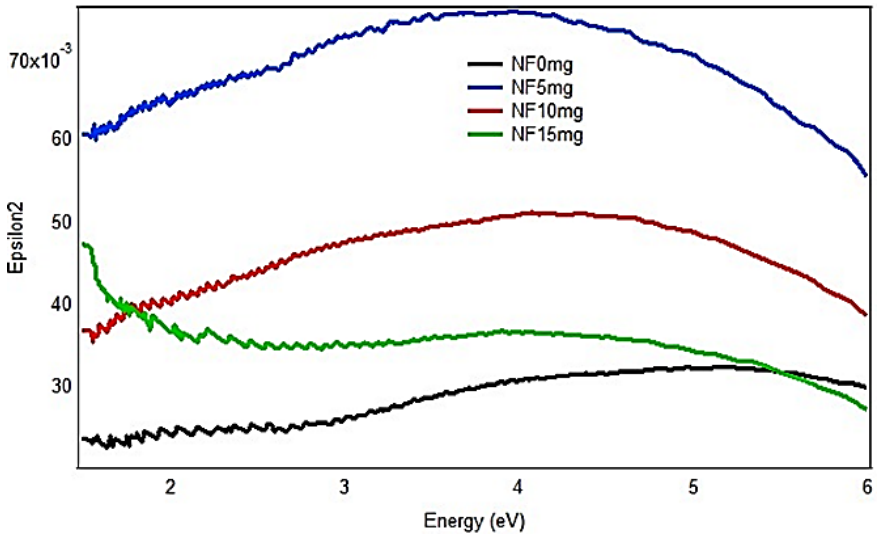


**Figure 8.** The imaginary part of dielectric constant of rGO/PVA nanofiber.

The results of the calculation of the complex dielectric constant showed in Fig. 7 and Fig. 8, respectively. It is shown that the profile of the real part of dielectric constant curve ($\varepsilon_1$) is similar to the real part of refractive index curve, that is, the value decreases significantly in the energy range below 2.3 eV with increasing rGO mass. In contrast to $\varepsilon_1$, the curve of the imaginary part of the dielectric constant ($\varepsilon_2$) appears to have increased quite significantly in the energy range lower than 2 eV. This is thought that the mass additional of rGO increases the conductivity of the rGO nanofiber.

Based on the data analysis that has been done, it is known that the morphology modification of rGO which is made into the nanofiber form gives quite an significant effect for the optical properties of the material, which makes rGO more transparent which characterized by decreasing optical absorption. Apart from that, the morphology of rGO being nanofiber makes its surface wider so it accommodates a lot electrons which in turn transition from the valence band to the conduction band easily making the rGO nanofiber even more conductive. Another possibility is caused by nanofiber structures are random and intersect each other at certain points thus makes it easier for electrons to transition at low energies. The characterization process that has been done, especially for the optical properties analyzed from the absorbance data, can be considered for the application of rGO nanofibers in organic solar cells as a transparent electrode layer.

## 4. Conclusion

In this study the rGO/PVA nanofibers were produced by electrospinning technique. Previously, the rGO used was obtained through a chemical reduction process using Hydrazine Hydrate to GO powder which firstly synthesized using the Hummer method with some modification. Furthermore, rGO was then formed into nanofibers with using PVA as a matrix polymer. The rGO nanofiber that was formed next characterized to determine its optical properties based on the absorbance data of the UV-Vis Spectrophotometry. Based on these data, it is known that the rGO/PVA nanofiber more transparent due to the addition of mass of rGO. Besides, it is also known that the addition of rGO mass is predicted to make the rGO/PVA nanofiber more conductive. These results make the rGO/PVA nanofiber ideal for application to transparent electrode layer on organic solar cells.

**Acknowledgment**

This work is based on research supported by Material Physics Laboratory, Physics Department and Integrated Research and Testing Laboratory (LPPT) of Universitas Gadjah Mada, Indonesia. Any opinion, findings, and conclusions described in this work are those of the authors. Financial support from Endowment Fund for Education (LPDP) of Indonesia on the research fund form.

**References**


[1] B. Mortazavi *et al.*, "Nanoporous graphene: A 2D semiconductor with anisotropic mechanical, optical and thermal conduction properties," *Carbon N. Y.*, vol. 147, pp. 377–384, 2019.

[2] S. N. Alam, N. Sharma, and L. Kumar, "Synthesis of graphene oxide (GO) by modified Hummers method and its thermal reduction to obtain reduced graphene oxide (rGO)," *Graphene*, vol. 6, no. 1, pp. 1–18, 2017.

[3] J. G.-Contreras and F. C.-Briones, "Graphene oxide powders with different oxidation degree, prepared by synthesis variations of the Hummers method," *Mater. Chem. Phys*., vol. 153, pp. 209–220, 2015.

[4] M. I. Katsnelson, *Graphene: Carbon in Two Dimensions*. Cambridge, USA: Cambridge University Press, 2012.

[5] K. Parvez *et al.*, "Exfoliation of graphite into graphene in aqueous solutions of inorganic salts," *J. Am. Chem. Soc.,* vol. 136, no. 16, pp. 6083–6091, 2014.

[6] K. Parvez, S. Yang, X. Feng, K. Mullen, "Exfoliation of graphene via wet chemical routes," *Synthetic Met.,* vol. 210, pp. 123–132, 2015.

[7] Y. Wei *et al.*, "Epitaxial growth of single-domain graphene on hexagonal boron nitride," *Nature Mater*, vol. 12, no. 9, pp. 792–797, 2013.

[8] H. Ago *et al.*, "Epitaxial growth and electronic properties of large hexagonal graphene domains on Cu(111) thin film," *Appl. Phys. Express,* vol. 6, no. 7, p. 075101, 2013.

[9] X. Yang *et al.*, "Chemical vapour deposition of graphene: layer control, the transfer process, characterization, and related applications," *Int. Rev. Phys. Chem.,* vol. 38, no. 2, pp. 149–199, 2019.

[10] H. Zhou *et al.*, "Chemical vapour deposition growth of large single crystals of monolayer and bilayer graphene," *Nat. Commun.,* vol. 4, no. 1, pp. 1–8, 2013.

[11] S. Some *et al.*, "High-quality reduced graphene oxide by a dual-function chemical reduction and healing process," *Sci. Rep.,* vol. 3, no. 1, pp. 1–5, 2013.

[12] F. T. Thema *et al.*, "Synthesis and characterization of graphene thin films by chemical reduction of exfoliated and intercalated graphite oxide," *J. Chem.*, vol. 2013, pp. 1–6, 2013.

[13] S. V. Tkachev *et al.*, "Reduced graphene oxide," *Inorg. Mater.,* vol. 48, no. 8, pp. 796–802, 2012.

[14] L. Stobinski *et al.*, "Graphene oxide and reduced graphene oxide studied by the XRD, TEM and electron spectroscopy methods," *J. Electron Spectroscopy and Related Phenomena,* vol. 195, pp. 145–154, 2014.

[15] H. Feng, R. Cheng, X. Zhao, X. Duan, and J. Li, "A low-temperature method to produce highly reduced graphene oxide," *Nat. Commun.,* vol. 4, no. 1, pp. 1–8, 2013.

[16] N. Cao and Y. Zhang, "Study of reduced graphene oxide preparation by Hummers' method and related characterization," *J. Nanomat.*, vol. 2015, pp. 1–5, 2015.

[17] K. W. Mas'udah, A. Taufiq, and Sunaryono, "A study on phase and microstructure of reduced graphene oxide prepared by heating corncobs," *JPSE (J. Phys. Sci. Eng.*), vol. 5, no. 2, pp. 66–70, 2020.

[18] B. Luo, S. Liu, and L. Zhi, "Chemical approaches toward graphene-based nanomaterials and their applications in energy-related areas," *Small,* vol. 8, no. 5, pp. 630–646, 2012.

[19] D. Zhang, F. Xie, P. Lin, and W. C. H. Choy, "Al-$TiO_2$ composite-modified single-layer graphene as an efficient transparent cathode for organic solar cells," *ACS Nano,* vol. 7, no. 2, pp. 1740–1747, 2013.

[20] G. H. Jun *et al.*, "Enhanced conduction and charge-selectivity by n-doped graphene flakes in the active layer of bulk-heterojunction organic solar cells," *Energy Environ. Sci.,* vol. 6, no. 10, pp. 3000–3006, 2013.

[21] S. Das *et al.*, "Electrospinning of polymer nanofibers loaded with noncovalently functionalized graphene," *J. Appl. Polym. Sci.,* vol. 128, no. 6, pp. 4040–4046, 2013.

[22] A. W. Rokmana *et al.*, "The optical properties of thin film reduced graphene oxide/poly (3,4 ethylenedioxtriophene): poly (styrene sulfonate) (PEDOT:PSS) fabricated by spin coating," *J. Phys.: Conf. Ser.,* vol. 1011, no. 1, p. 012007, 2018.

[23] H. Suhendar, A. Kusumaatmaja, K. Triyana, and I. Santoso, "Effect of chemical reduction temperature on optical properties of reduced graphene oxide (rGO) and its potentials supercapacitor device," *Mat. Sci. Forum,* vol. 901, pp. 55–61, 2017.

[24] J. Chen, B. Yao, C. Li, and G. Shi, "An improved Hummers method for eco-friendly synthesis of graphene oxide," *Carbon,* vol. 64, pp. 225–229, 2013.
[25] M. Fox, *Optical Properties of Solids.* New York: New Oxford University Press, 2001.
[26] L. Shahriary and A. A. Athawale, "Graphene oxide synthesized by using modified Hummers approach," *Int. J. Renewable Energy and Env. Eng.,* vol. 2, no. 1, pp. 58–63, 2014.
[27] B. Q. Bao *et al.*, "Graphene-polymer nanofiber membrane for ultrafast photonics," *Adv. Funct. Mater.,* vol. 20, no. 5, pp. 782–791, 2010.
[28] L. Jin *et al.*, "Fabrication, mechanical properties, and biocompatibility of reduced graphene oxide-reinforced nanofiber mats," *RSC Adv.,* vol. 4, no. 66, pp. 35035–35041, 2014.